JACS
JOURNAL OF THE AMERICAN CHEMICAL SOCIETY

Communication

pubs.acs.org/JACS

Structural Mimics of Viruses Through Peptide/DNA Co-Assembly

Rong Ni[†] and Ying Chau*[,†,‡]

[†]Department of Chemical and Biomolecular Engineering and [‡]Division of Biomedical Engineering, The Hong Kong University of Science and Technology, Clear Water Bay, Kowloon, Hong Kong, China

Supporting Information

ABSTRACT: A synthetic mimic of viral structure has been constructed by the synergistic co-assembly of a 16-amino acid peptide and plasmid DNA. The rational design of this short peptide, including segments for binding DNA and forming β-sheet, is inspired by viral capsid protein. The resulting nanostructures, which we term nanococoons, appear as ellipsoids of virus-like dimension (65 × 47 nm) and display repeating stripes of ~4 nm wide. We propose that the co-assembly process involves DNA as a template to assist the organization of peptide strands by electrostatic interaction, while the bilayer β-sheets and their lateral association stabilize the peptide "capsid" and organize the DNA within. The hierarchy affords an extremely stable structure, protecting peptide and DNA against enzymatic digestion. It opens a new and facile avenue to fabricate viral alternatives with diverse functions.

Nature-inspired nanotechnology has been pursued for decades due to the efficient strategies developed by nature to build complex systems with simple building blocks.[1,2] Viruses, as naturally evolved products, are assembled by protein and nucleic acid. Their sophisticated nanostructures and unique surface patterns have been used as structural templates to build functional materials and adopted as vectors for gene delivery.[3−5] There has been increasing interest in creating virus-like particles via genetically engineered protein units[6] and fabricating nanocarriers for gene delivery using polycations.[7−9] However, the elegance and simplicity of forming viral nanostructures have not been replicated by synthetic materials. Herein, a short peptide with viral capsid protein-like functions has been designed. The peptides were used as building blocks to co-assemble with pDNA into virus-like nanoparticles with well-defined surface patterns.

In spite of the diversity in morphologies and functions of viruses, their capsid proteins usually share a common structural motif. It consists of: (1) a positively charged region to interact with genes, (2) a hydrophobic region to stabilize the whole capsid through secondary structure and noncovalent interaction among neighboring units, and (3) a hydrophilic segment to stabilize virions in solution.[10,11] To mimic the viral capsid protein, we have constructed a short peptide of 16 amino acid residues, named K_3C_6SPD (Figure 1A), which includes three segments: (1) an N-terminal DNA-binding oligocation, (2) a central short hydrophobic β-sheet forming segment derived from the hydrophobic region of Amyloid β peptide (Aβ(17−21)),[12] and (3) a C-terminal hydrophilic segment. In addition, a flexible alkyl linker (C_6) and a short glycine linker are added

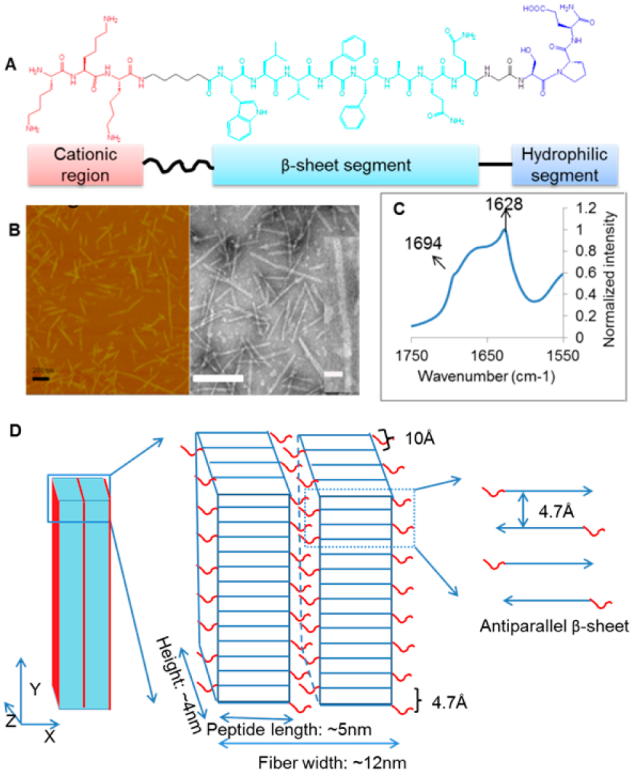

Figure 1. (A) Primary structure of K_3C_6SPD. The peptide consists of three modular segments as labeled. (B) AFM (left, scale bar = 200 nm) and TEM (right, scale bar = 100 nm) images of the K_3C_6SPD nanoribbons. The inset shows an image of a single K_3C_6SPD nanoribbon (scale bar = 20 nm). (C) Amide I region on the FTIR spectrum of K_3C_6SPD nanoribbons. (D) The antiparallel bilayer structure model of the K_3C_6SPD nanoribbon, showing lysine in red and the rest of K_3C_6SPD in blue. X, Y, and Z represent directions along the peptide backbone, H-bonding, and lamination, respectively.

to the N- and C-terminus of segment 2, respectively, to allow for conformational freedom. Two glutamines are introduced next to the β-sheet segment to promote peptide aggregation by side-chain hydrogen bonding.[13] A tryptophan residue is embedded at the N-terminus of the β-sheet segment as a fluorescent probe for monitoring changes in the structure and local environment during the peptide assembly process.[14]

In aqueous phase and at neutral pH, K_3C_6SPD at 0.20 mM assembled into filamentous nanoribbons of ~4 nm in height

Received: July 31, 2014
Published: November 12, 2014

   dx.doi.org/10.1021/ja507833x | J. Am. Chem. Soc. 2014, 136, 17902−17905

and ~12 nm in width (Figures 1B and S1A–C). Study of concentration dependence showed that K_3C_6SPD at a concentration as low as 0.05 mM assembled into nanoparticles of ~12 nm in diameter; and once the concentration was over 0.10 mM, short nanoribbons started to form (Figure S1D–J). Circular dichroism (CD) analysis of matured K_3C_6SPD nanoribbons yielded the signature β-sheet spectra with main negative ellipticity centered at 215 nm. A negative shoulder peak at 228 nm, frequently cited for tryptophan-present peptide, was observed (Figure S2A).[15] Fourier transform infrared spectroscopy (FTIR) showed the amide I stretch at 1628 cm^{-1} and a high wavenumber shoulder band around 1694 cm^{-1}, revealing the antiparallel β-sheet architecture within the nanoribbons (Figure 1C).[16] K_3C_6SPD is around 5 nm in length by calculation (see Supporting Information), which is about half the observed width of the nanoribbon (12 nm), thereby suggesting a bilayer structure. X-ray powder diffraction defined an H-bonding distance of 4.7 Å and a lamination distance of 10.3 Å (Figure S2B), consistent with observations in other Aβ-peptide assemblies.[17] By considering the above information, we propose a bilayer structure for K_3C_6SPD nanoribbons (Figure 1D). In this model, half of the N-terminal lysine and tryptophan residues are exposed to the aqueous phase, which would give rise to a positively charged nanoribbon surface and provide a hydrophilic environment for the tryptophan residues. We did find the ζ potential of nanoribbons to be around +20 mV and the maximal fluorescence emission of tryptophan at 357 nm (Figure S2C). Antiparallel β-sheet bilayer architecture has also been observed in nanofibers and nanotubes assembled by the same β-sheet region of Aβ(17–21),[17,18] suggesting that this region dominates K_3C_6SPD self-assembly and drives the peptide organization.

By the addition of K_3C_6SPD (0.20 mM) into diluted DNA solution (10 μg/mL) at an N/P ratio of 20, ellipsoid-shaped nanoparticles of ~65 × 47 nm were observed. They appeared as singlets as well as doublets, triplets, and agglomerations of even a higher degree (Figures 2A–C and S3A). These particles are morphologically similar to parapoxvirus, which has a characteristic cocoon-like shape and a striped surface pattern.[19] We name the new nanoparticles as nanococoons. The stripes on the nanococoon surface are ~4 nm in width, reminiscent of the dimension found in the bundled nanoribbons through lateral association (Figure 2B). The height of dried nanococoons, estimated from AFM images, is ~24 nm (Figure 2C), suggesting a capsule-like core of the nanococoons. Chemical component analysis of these nanococoons by time-of-flight secondary ion mass spectrometry (TOF-SIMS) (Figure 2D) confirmed the colocalization of DNA (by the detection of PO_3^- ions) and K_3C_6SPD (by CNO^-).[20] Thus, the nanococoons are derived from the co-assembly of K_3C_6SPD and DNA.

Similarity in the striped patterns for the nanococoons and the bundled nanoribbons suggests that K_3C_6SPD may share the same organization at the molecular level. It appears that K_3C_6SPD nanoribbons form an outer coat bundling around DNA, similar to how the viral capsid proteins are structured around the genome. This hypothesis was supported by the following evidences. First, FTIR showed an amide I band of 1628 cm^{-1} and a high-wavenumber shoulder band of 1694 cm^{-1}, which are identical to those of nanoribbons in the absence of DNA (Figure S3D), suggesting that K_3C_6SPD on the nanococoon adopts the same antiparallel β-sheet architecture. Next, X-ray powder diffraction gave the same H-bonding distance (4.7 Å) and lamination spacing (10 Å) for the

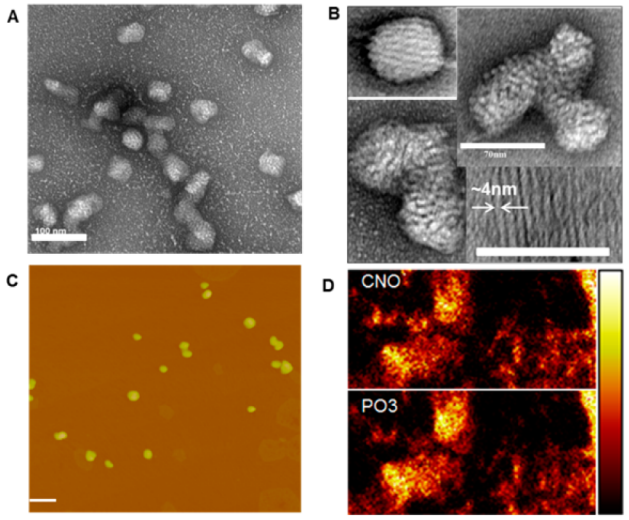

Figure 2. (A) TEM image of a population of K_3C_6SPD/DNA nanococoons (scale bar = 100 nm). (B) TEM images of nanococoons appearing as a singlet, doublet, and triplet. Image of the bundled K_3C_6SPD nanoribbons (scale bar = 70 nm). (C) AFM image of K_3C_6SPD/DNA nanococoons (scale bar = 200 nm). (D) TOF-SIMS mass-resolved images of negatively charged secondary ions CNO^- from K_3C_6SPD and PO_3^- from DNA in an area of 21.5 × 10.8 μm^2.

K_3C_6SPD "capsid" (Figure S3E). In addition, tryptophan residues in these nanococoons were exposed to a local environment similar to the nanoribbons, with a maximal emission at 357 nm (Figure S2C). Moreover, the surface of nanococoons was positively charged, as shown by ζ potential (+25 mV) and by binding with negatively charged nanogold colloids (Figure S3B). If our hypothesis is correct, these nanococoons could be formed by mixing preformed nanoribbons with plasmid DNA. Indeed, we observed striped nanoparticles with free ribbons extruding outward (Figure S3C), while the co-assembly of K_3C_6SPD monomers and DNA generated a striped but smooth surface. These evidences suggest that K_3C_6SPD assembles into nanoribbons in the presence of DNA and simultaneously wraps around DNA, resulting in the formation of nanococoons.

In these co-assembled nanococoons, K_3C_6SPD and DNA strongly interact with each other to afford stable nanostructures, which are extremely resistant to enzyme digestion. In agarose gel electrophoresis, DNA was found to be completely retarded, suggesting the condensation of DNA by the K_3C_6SPD "capsid" (Figure 3A). Upon brief DNase I treatment, naked DNA was completely degraded; while the K_3C_6SPD/DNA nanococoons were intact even after prolonged enzymatic treatment (Figure 3B).[21] In addition, trypsin and chymotrypsin digestion of K_3C_6SPD in the nanococoons caused negligible effects on the particles (DLS data not shown), implying that the cleavage sites are inaccessible to both peptidases due to the compact structure of nanococoons. Regarding the enzyme impermeability and gene protection, these nanococoons imitate the advantages of viruses.[22] Previous studies have demonstrated that when there is merely electrostatic interaction between peptide and DNA, three lysines are too short to form a stable complex with DNA.[23] Therefore, the high stability of nanococoons suggests that the secondary structure and lateral association of the nanoribbons play important roles in stabilizing the K_3C_6SPD "capsid" formation, mimicking the tight interaction among virion capsid proteins in nature. Thus,

dx.doi.org/10.1021/ja507833x | J. Am. Chem. Soc. 2014, 136, 17902–17905

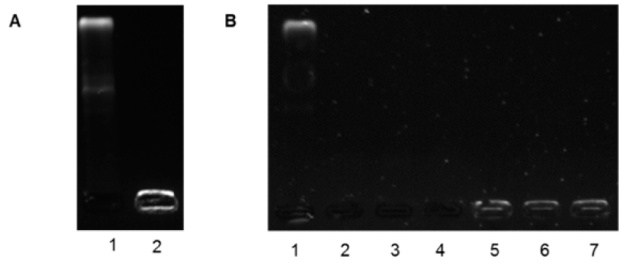

Figure 3. (A) Agarose gel image of free DNA (lane 1) and DNA encapsulated by nanococoons (lane 2). (B) DNase I digestion assay. Lane 1: DNA control without DNase I treatment. Lanes 2–4 are the naked DNA treated with DNase I for 15, 30, 45 min, respectively. Lanes 5–7 are nanococoons treated with DNase I for 15, 30, 45 min, respectively.

these nanococoons are superior to most polycation and peptide-based artificial viruses by leveraging the nanostructure for protective functions.[7−9] The artificial virus recently reported by Lee's group[24] consisted of siRNA adhering to the outer surface of preformed peptide nanoribbons, rather than building a protective peptide shell around the genetic materials.

Taking all the information above, we propose a structural model for the nanococoon (Figure 4). Once K_3C_6SPD monomers are mixed with DNA, they are preorganized along the DNA backbone by electrostatic interaction; such an organization assists their self-assembly into nanoribbons. The nanoribbons are laterally associated and form the distinct stripes of the "capsid"; this ordering helps to condense and organize DNA inside the nanococoon. At the molecular level, we assume that the H-bonding direction is along the DNA backbone and all the phosphate charges of DNA are neutralized by the amines of K_3C_6SPD. The H-bonding distance in the β-sheet is 4.7 Å, and the spacing between phosphate groups along a DNA chain is 3.4 Å; so approximately every two K_3C_6SPD strands along the H-bonding direction would interact with three phosphate groups. Note that the antiparallel β-sheet architecture only permits one of two K_3C_6SPD strands to neutralize three consecutive phosphate groups. In the lamination direction, five laminates with 10 Å interval are proposed according to the width of strips (~4 nm) (top view, Figure 4). In each laminate, two K_3C_6SPD strands stack to form a bilayer structure, giving a height of ~12 nm. The surface distribution of positive charges is illustrated in the side-view, in which the proposed interaction between lysines of K_3C_6SPD strands and the phosphate groups of DNA is mapped. In this model, every repeating unit includes 6 phosphate groups and 20 K_3C_6SPD strands in a 5 laminated antiparallel bilayer structure (5 × 4) (side-view in Figure 4). Since each K_3C_6SPD bears three net positive charges, an N/P ratio of 10 is predicted for charge neutralization.

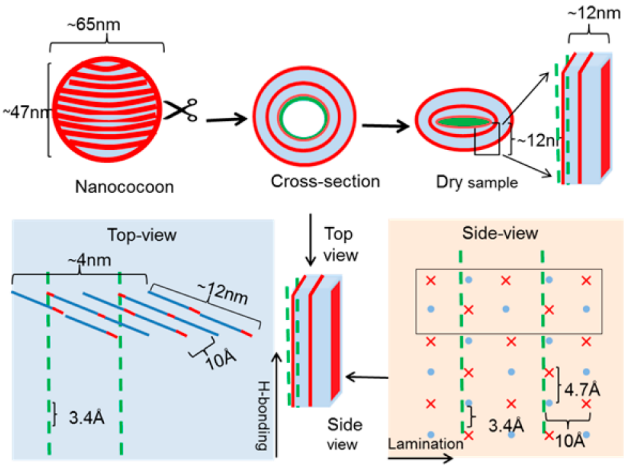

Figure 4. Structural model of the K_3C_6SPD/DNA nanococoon. The cross-section shows the bilayer structure of K_3C_6SPD "capsid" and the organized DNA inside. The top view shows that K_3C_6SPD strands form antiparallel β-sheets and adopt a bilayer structure. Lysines are shown in red and the rest of the K_3C_6SPD in blue. The side view maps the interaction between K_3C_6SPD and DNA duplex shown in green. Green slash line: phosphate group; red-cross: lysine; blue dot: C-terminus of K_3C_6SPD, displayed on the outer surface of the stripes.

An N/P ratio of 10 represents the minimum requirement for K_3C_6SPD to interact with DNA if all phosphate groups are neutralized by the amines as proposed in the above model. To evaluate this model, K_3C_6SPD at different concentrations was co-assembled with DNA (10 μg/mL) to achieve different N/P ratios. At an N/P ratio of 5 (0.05 mM K_3C_6SPD), big amorphous aggregates without obvious striation were observed (Figure 5A). When the N/P ratio was increased to 10 (0.10 mM K_3C_6SPD), agglomerations with small striped nanococoons were formed (Figure 5B). At an N/P ratio of 15 and 20 (0.15 mM and 0.20 mM K_3C_6SPD), well dispersed and mostly homogeneous nanococoons were generated (Figure 5C, D). Further increase of the N/P ratio to 25 and 50 (0.25 mM and 0.50 mM K_3C_6SPD) resulted in the co-existence of striped nanococoons and filamentous nanoribbons (Figure 5E, F). Surface analysis identified a differentially charged surface, with ζ potential of +16 mV and +25 mV for agglomerated and well-dispersed nanococoons, respectively. This difference may account for the distinct dispersion state of nanococoons at the N/P of 10 and 20.[25,26] In addition, fluorescence analysis confirmed that the tryptophan residues were buried in a more hydrophobic environment in the big agglomeration than the small nanococoons. However, on the structural aspect, K_3C_6SPD in these big agglomeration and nanococoons shared the same β-sheet secondary structure and d-spacings (Figure S4). These findings imply that K_3C_6SPD strands are pre-organized in a similar way on DNA surface at both N/P ratios.

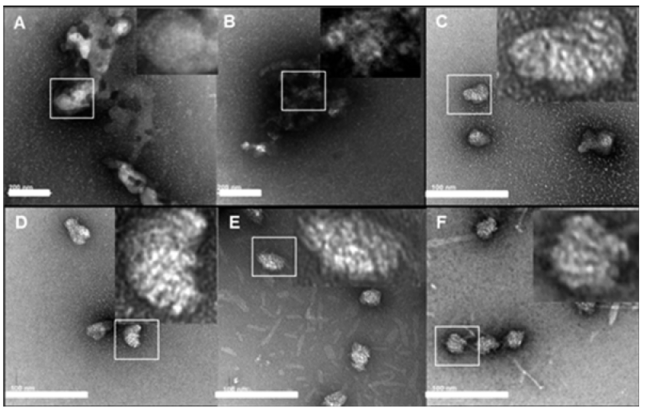

Figure 5. TEM images of K_3C_6SPD/DNA nanoparticles at different N/P ratios: (A) 5 (0.05 mM K_3C_6SPD), (B) 10 (0.10 mM K_3C_6SPD), (C) 15 (0.15 mM K_3C_6SPD), (D) 20 (0.20 mM K_3C_6SPD), (E) 25 (0.25 mM K_3C_6SPD), and (F) 50 (0.50 mM K_3C_6SPD). The insets show the zoomed-in images of the highlighted nanococoons. Scale bar = 200 nm.

dx.doi.org/10.1021/ja507833x | J. Am. Chem. Soc. 2014, 136, 17902−17905

An N/P ratio of 10 provides the minimum amount of K_3C_6SPD to assemble into nanoribbons and sufficient charges to neutralize DNA. Extra K_3C_6SPD strands are required for the formation of well-dispersed nanococoon; an N/P ratio of 20 supplies the optimal amount of K_3C_6SPD in this co-assembly process.

In summary, we successfully developed cocoon-like structural mimics of viruses with ordered striped "capsids". The mimic is morphologically similar to the parapoxvirus. The K_3C_6SPD "capsid", stabilized by β-sheets, shows robustness and low permeability to enzymes, thus imitating viral capsid on the architecture and the function of gene protection.[10,22] Involvement of peptide secondary structure in this nanococoon fabrication complements the work of previously reported artificial viruses, which were constructed by electrostatically complexing DNA with large polycations negating the formation of ordered protective capsid.[8,9,27] Peptide/DNA interaction during the nanococoon formation in this simple system provides a feasible model to understand gene condensation and encapsulation during the origin of virion at the prebiotic age. Understanding of this co-assembly process would offer the capability to regulate and control the properties of this viral mimic by the facile introduction of functional groups into building blocks. This work therefore enriches the tool box to build functional peptide/DNA based nanomaterials and opens a new avenue to construct virus-inspired therapeutics.

■ ASSOCIATED CONTENT

Supporting Information

Experimental details and supplemental figures. This material is available free of charge via the Internet at http://pubs.acs.org.

■ AUTHOR INFORMATION

Corresponding Author

keychau@ust.hk

Notes

The authors declare no competing financial interest.

■ ACKNOWLEDGMENTS

The authors acknowledge the support from the Hong Kong Research Grant Council (GRF660211). The authors thank the support from Materials Characterization & Preparation Facility for AFM and TEM usage as well as TOF-SIMS sample analysis and also the support from Biosciences Central Research Facility for peptide characterization.

■ REFERENCES

(1) Liu, N.; Lu, Z.; Zhao, J.; McDowell, M. T.; Lee, H. W.; Zhao, W.; Cui, Y. *Nat. Nanotechnol.* **2014**, *9*, 187.

(2) Bar-Cohen, Y. *Proc. SPIE* **2012**, *8482*; DOI 10.1117/12.928048.

(3) Chen, P. Y.; Dang, X. N.; Klug, M. T.; Qi, J. F.; Courchesne, N. M. D.; Burpo, F. J.; Fang, N.; Hammond, P. T.; Belcher, A. M. *ACS Nano* **2013**, *7*, 6563.

(4) Gorzny, M. L.; Walton, A. S.; Evans, S. D. *Adv. Funct Mater.* **2010**, *20*, 1295.

(5) Lentz, T. B.; Gray, S. J.; Samulski, R. J. *Neurobiol. Dis.* **2012**, *48*, 179.

(6) Cadena-Nava, R. D.; Comas-Garcia, M.; Garmann, R. F.; Rao, A. L. N.; Knobler, C. M.; Gelbart, W. M. *J. Virol.* **2012**, *86*, 3318.

(7) Mannisto, M.; Vanderkerken, S.; Toncheva, V.; Elomaa, M.; Ruponen, M.; Schacht, E.; Urtti, A. *J. Controlled Release* **2002**, *83*, 169.

(8) Lungwitz, U.; Breunig, M.; Blunk, T.; Gopferich, A. *Eur. J. Pharm. Biopharm.* **2005**, *60*, 247.

(9) Mao, H. Q.; Roy, K.; Troung-Le, V. L.; Janes, K. A.; Lin, K. Y.; Wang, Y.; August, J. T.; Leong, K. W. *J. Controlled Release* **2001**, *70*, 399.

(10) *Advances in Virus Research, Virus Structure and Assembly*; Elsevier Academic Press: San Diego, CA, 2005; Vol. *64*.

(11) Mathieu, M.; Petitpas, I.; Navaza, J.; Lepault, J.; Kohli, E.; Pothier, P.; Prasad, B. V. V.; Cohen, J.; Rey, F. A. *EMBO J.* **2001**, *20*, 1485.

(12) Luhrs, T.; Ritter, C.; Adrian, M.; Riek-Loher, D.; Bohrmann, B.; Dobeli, H.; Schubert, D.; Riek, R. *Proc. Natl. Acad. Sci. U.S.A.* **2005**, *102*, 17342.

(13) Plumley, J. A.; Dannenberg, J. J. *J. Am. Chem. Soc.* **2010**, *132*, 1758.

(14) Pattanaik, P.; Ravindra, G.; Sengupta, C.; Maithal, K.; Balaram, P.; Balaram, H. *FEBS J.* **2003**, *270*, 745.

(15) Bishop, C. R.; Walkenhorst, W. F.; Wimley, W. C. *J. Mol. Biol.* **2001**, *309*, 975.

(16) Cerf, E.; Gustot, A.; Goormaghtigh, E.; Ruysschaert, J. M.; Raussens, V. *FASEB J.* **2011**, *25*, 1585.

(17) Childers, W. S.; Mehta, A. K.; Ni, R.; Taylor, J. V.; Lynn, D. G. *Angew. Chem., Int. Edit* **2010**, *49*, 4104.

(18) Ni, R.; Childers, W. S.; Hardcastle, K. I.; Mehta, A. K.; Lynn, D. G. *Angew. Chem., Int. Edit* **2012**, *51*, 6635.

(19) Nollens, H. H.; Jacobson, E. R.; Gulland, F. M. D.; Beusse, D. O.; Bossart, G. D.; Hernandez, J. A.; Klein, P. A.; Condit, R. C. *J. Wildlife Dis.* **2006**, *42*, 23.

(20) Wang, W. P.; Chau, Y. *Soft Matter* **2009**, *5*, 4893.

(21) Bordelon, H.; Biris, A. S.; Sabliov, C. M.; Monroe, W. T. *J. Nanomater.* **2011**, *2011*, 1.

(22) Carter, J. B. a. S, V. A. *Virology principles and applications*; John Wiley & Sons, Ltd: Chichester, 2007.

(23) Kwoh, D. Y.; Coffin, C. C.; Lollo, C. P.; Jovenal, J.; Banaszczyk, M. G.; Mullen, P.; Phillips, A.; Amini, A.; Fabrycki, J.; Bartholomew, R. M.; Brostoff, S. W.; Carlo, D. J. *Biochim. Biophys. Acta, Gene Struct. Expression* **1999**, *1444*, 171.

(24) Lim, Y. B.; Lee, E.; Yoon, Y. R.; Lee, M. S.; Lee, M. *Angew. Chem., Int. Edit* **2008**, *47*, 4525.

(25) Graf, C.; Gao, Q.; Schutz, I.; Noufele, C. N.; Ruan, W. T.; Posselt, U.; Korotianskiy, E.; Nordmeyer, D.; Rancan, F.; Hadam, S.; Vogt, A.; Lademann, J.; Haucke, V.; Ruhl, E. *Langmuir* **2012**, *28*, 7598.

(26) Lebovka, N. I. *Adv. Polym. Sci.* **2014**, *255*, 57.

(27) Tonges, L.; Lingor, P.; Egle, R.; Dietz, G. P. H.; Fahr, A.; Bahr, M. *RNA* **2006**, *12*, 1431.